ELECTRONIC SUPPLEMENTARY INFORMATION

Multifunctional Hydroxyquinoline-Derived Turn-on Fluorescent Probe for Alzheimer's Disease Detection and Therapy

Priyam Ghosh,[1] Sayantani Mukhopadhyay,[2] Thirukumaran Kandasamy,[3] Subrata Mondal,[1] Siddhartha Sankar Ghosh,[2,3,4] and Parameswar Krishnan Iyer[1,2,4]*

[1]Department of Chemistry, Indian Institute of Technology Guwahati, Guwahati-781039, Assam, India.

[2]Center for Nanotechnology, Indian Institute of Technology Guwahati, Guwahati-781039, Assam, India.

[3]Department of Bioscience and Bioengineering, Indian Institute of Technology Guwahati, Guwahati-781039, Assam, India.

[4]Jyoti and Bhupat Mehta School of Health Science and Technology, Indian Institute of Technology Guwahati, Guwahati 781039, Assam, India.

Email: pki@iitg.ac.in

TABLE OF CONTENT

1. Materials and Methods:

All the reagents were purchased from Sigma Aldrich and were not refined before use. For the experiments, Milli-Q water and solvents of HPLC grade were used. Amyloid-β 16-21 (Aβ16-21) and Amyloid-β 1-40 peptide fragment (Aβ40) were acquired from Biotech Desk Pvt. Ltd. in Hyderabad, India. Lysotracker green was purchased from Abcam. LAMP-1 and β-actin 1˚-antibody were purchased from Cell Signalling Technology. Borosil microscope glass slides were used for microscopy.

2. Instrumentation:

UV-Vis spectra were recorded using Perkin Elmer Lambda 365+ spectrometer. The fluorescence spectra were recorded using a Horiba Scientific Fluoromax-4 Spectrofluorometer equipped with a xenon lamp under Room temperature conditions. The slit widths were set to 5 nm, and the measurements were conducted in a quartz cuvette with a path length of 1 cm. Excitation wavelengths and other parameters, such as solvent details and pH, have been included in the revised manuscript for clarity. 400 MHz FT NMR, Make: Bruker, Model: AVANCE 400. HPLC data was recorded in a thermos scientific instrument, Make: Dionex Softron GmbH, Germany; Eclipse Plus C18 5 um column was used to check the analytical purity of the sample. TEM images were recorded by JEOL 2100 transmission electron microscope. Crystal data were taken in Single Crystal X-ray Diffractometer, Make: Agilent, Model: Single source supernova E (Mo source). ITC data were recorded in Isothermal Titration Calorimeter, Make: GE Health Care, Model: iTC 200 Micro-calorimeter. MALDI data were recorded in Matrix-Assisted Laser Desorption/Ionization Time of Flight, Make: BRUKER Model: AUTOFLEX SPEED. Colocalization data was recorded using Confocal Microscope, Make: Zeiss Model: LSM880. XPS data were recorded using an XPS instrument, Make: Physical Electronics, USA, Model: PHI 5000 Versa Probe III, Xray Source: monochromated K-Alpha (1486.7 eV), Focus: <10 μm to 300 μm.

3. Characterization of M8HQ:

NMR data of M8HQ:

Light yellow powder (70% yield)

^{1}H NMR (400 MHz, $CDCl_3$) δ 8.90, 8.88, 8.86, 8.85, 8.68, 8.66, 8.39, 8.37, 8.28, 8.26, 7.83, 7.81, 7.79, 7.62, 7.60, 7.58, 7.50, 7.49, 7.48, 7.47, 7.47, 7.26, 6.75, 6.73, 4.27, 4.25, 4.23, 3.63, 3.62, 3.61, 2.52, 2.50, 2.48, 2.44, 1.95, 1.93, 1.92, 1.69.

^{1}H NMR (400 MHz, $CDCl_3$) δ 8.87 (dd, *J* = 13.4, 6.2 Hz, 2H), 8.67 (d, *J* = 7.2 Hz, 1H), 8.38 (d, *J* = 8.2 Hz, 1H), 8.27 (d, *J* = 8.5 Hz, 1H), 7.81 (t, *J* = 7.6 Hz, 2H), 7.60 (t, *J* = 7.9 Hz, 1H), 7.52 – 7.44 (m, 2H), 6.74 (d, *J* = 8.3 Hz, 1H), 4.27 – 4.20 (m, 2H), 3.66 – 3.57 (m, 4H), 2.51 – 2.40 (m, 6H), 1.96 – 1.89 (m, 2H).

^{13}C NMR (151 MHz, $CDCl_3$) δ 164.73, 164.07, 160.66, 151.19, 150.98, 141.39, 136.45, 132.89, 132.02, 130.31, 129.91, 129.32, 126.92, 126.70, 125.69, 124.02, 122.77, 122.34, 120.34, 116.86, 111.47, 77.41, 77.20, 76.99, 67.16, 56.72, 53.75, 38.95, 24.89.

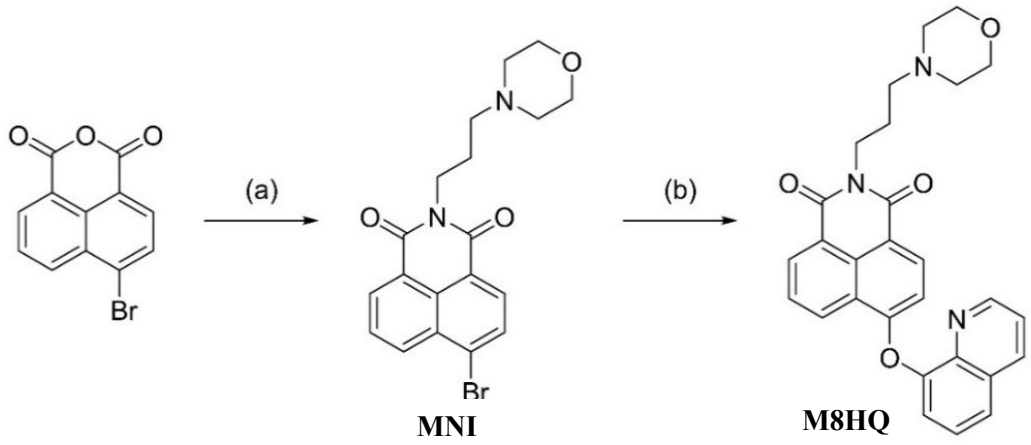

(a) 3-Morpholinopropylamine, ethanol, 85 °C; 12 h. (b) 8-Hydroxyquinoline, K_2CO_3, DMF, 95 °C, 24 h.

Scheme S1: Synthesis scheme of M8HQ

4. Molecular Docking Study:

A docking study was conducted using AutoDock and AutoDock Vina. The crystal structure of the M8HQ ligand was first optimized using AutoDock tools. Subsequently, the atomic resolution structure of the Aβ42 fibril was retrieved from the RCSB PDB databank (PDB ID 2NAO). Polar hydrogen was then added to the protein using AutoDock tools. Precise docking was performed on each part of the Aβ42 assembly to identify the most probable binding sites. The grid dimension was set to 50 × 50 × 50 Å, and the Lamarckian Genetic Algorithm was utilized for the process, with all other parameters maintained at their default settings. Finally, the docking results were analyzed using Discovery Studio 2021.

5. Stock Solution Preparation:

- Stock Solution of M8HQ: The appropriate amount of solid M8HQ powder was dissolved in DMSO and then diluted to create a 10 mM M8HQ solution as needed. A vortex mixer was used to ensure complete dissolution.
- Stock Solution of Aβ40 monomer: Aβ40 was treated with 1,1,1,3,3,3-hexafluoro-2-propanol (HFIP) and trifluoroacetic acid (TFA) to remove any pre-existing aggregates. Firstly, 10 µL of TFA was used to treat 1 mg of Aβ40, which was then dried in argon. Subsequently, 10 µL of HFIP was added to the solution, which was again dried in argon. Finally, to obtain a 230 µM stock Aβ40 monomer, 1 ml of a 10 mM PBS solution was added to the solution.
- Preparation of Aβ40 aggregates: To prepare Aβ aggregates, Aβ stock solution was diluted to 50 µM with pre-cooled 10 mM PBS buffer solution and centrifuged under 16000 × g for 10 min. to obtain the 50 µM monomer and then it was incubated at 37°C with a constant stirring (500 rpm) for 3 days.

6. M8HQ induced Aβ aggregation and Cu(II) interaction:

Field Emission Transmission Electron Microscopy:

Field-Emission Transmission Electron Microscopy (FETEM) samples (50 µM) were prepared by depositing 10 µL of the appropriate solution onto a carbon-coated copper grid for 5 mins, absorbing the excess solution with a small piece of filter paper. Then, 5 µL of Uranyl acetate (2%) contrasting agent solution was added to the grid. The liquid on the grid was then gently soaked after 3 minutes using a corner of filter paper, and the resulting grid was then dried in the air for an additional 3-4 hours. With the advantage of a JEOL 2100 electron microscope, the TEM images were captured.

Interaction of Amyloid-β Peptide Using MALDI:

By using matrix-assisted laser desorption ionization time-of-flight (MALDI-TOF) spectrometry, it was possible to determine how M8HQ and Cu^{2+} affected the aggregation of the Aβ40 peptide over time. In PBS, pH 7.4, at 37°C, Aβ40 peptide (100 µM) and M8HQ (1 mM) were incubated for 24 hours. A saturated solution of α-cyano-4-hydroxycinnamic acid was used to create the matrix (CHCA). By dissolving 10 mg in 1 ml of 70 % ACN:30 % of 0.1 % TFA in Milli-Q water, a saturated solution of CHCA was created. A 1:1 mixture of Aβ 40

peptide samples and matrix was used to spot the samples onto metal plates, let them air dry for 20 minutes, and then analyze the results using a MALDI-TOF spectrometer.

7. Fluorescence Measurement:

10 mM DMSO concentrated stock solution is made from M8HQ powder. To determine the probe's photostability, a solution of M8HQ (10 µM) in DMSO was continually exposed to 370 nm excitation light for 30 minutes. M8HQ were added to the freshly prepared Aβ40 (10 µM) sample in PBS buffer (10 mM, pH 7.4). The mixtures were vortexed and incubated at 37 °C for 24 h. The extent of fibril formation was quantified by ThT binding assay. For the copper-induced Aβ40 aggregation inhibition study, M8HQ (20 µM) was added to Aβ40 (10 µM) in PBS independently and incubated at 37 °C for 24 h; the samples were then analyzed by ThT binding assay. ThT (10−20 µM) was added at the end of the experiment, and fluorescence was recorded at 480 nm (λ_{ex} = 450 nm).

8. Figures:

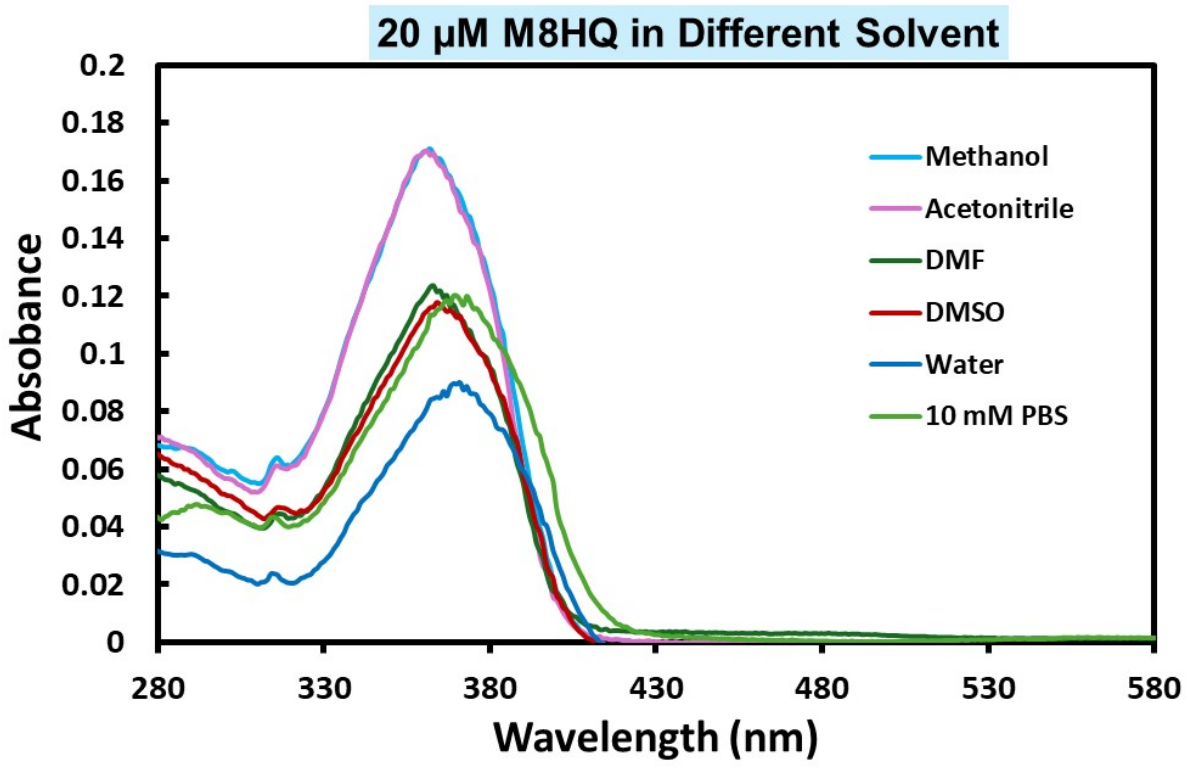

Figure S1: UV-Vis absorption spectra of 20 µM M8HQ obtained from different solvents. DMSO has been used as a stock solution.

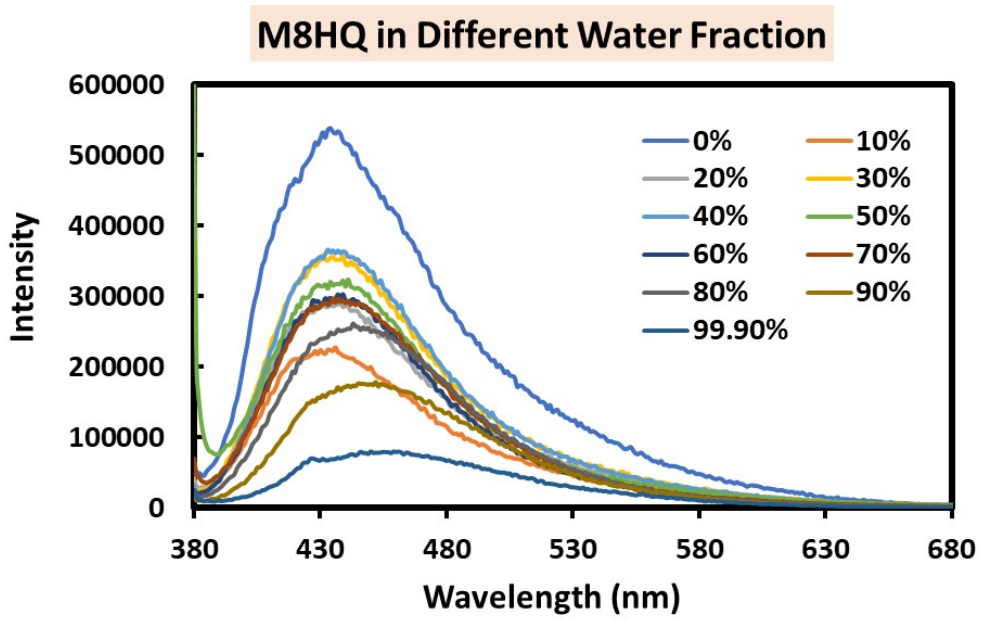

Figure S2: Fluorescence spectra of 20 µM M8HQ obtained from different water fractions. DMSO has been used as a stock solution.

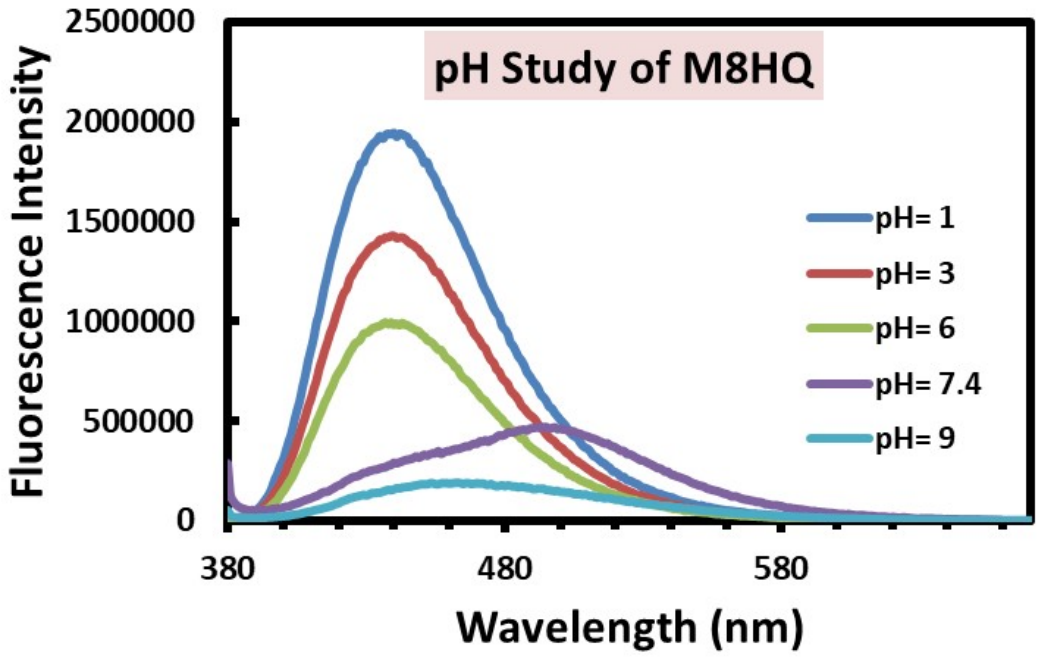

Figure S3: Fluorescence spectra of 20 µM M8HQ in different pH conditions.

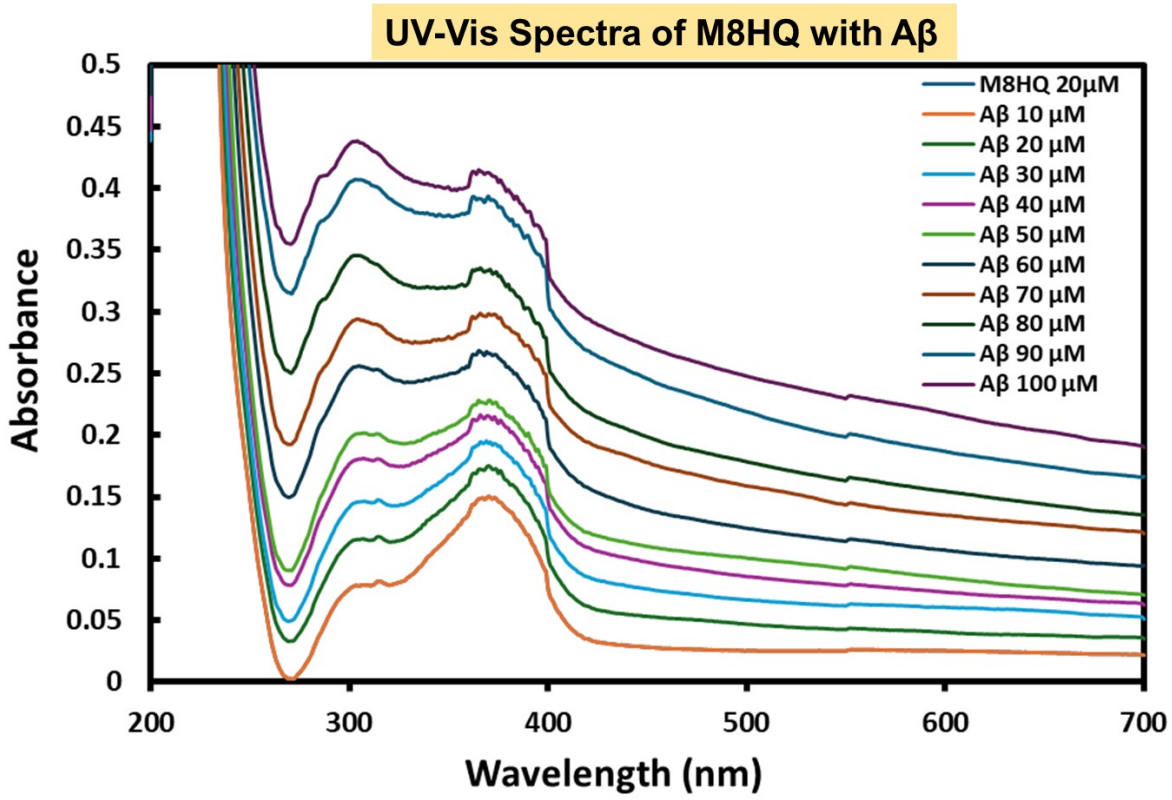

Figure S4: UV-Vis spectra of 20 µM M8HQ with increasing concentrations of Aβ40 peptide (10 to 100 µM).

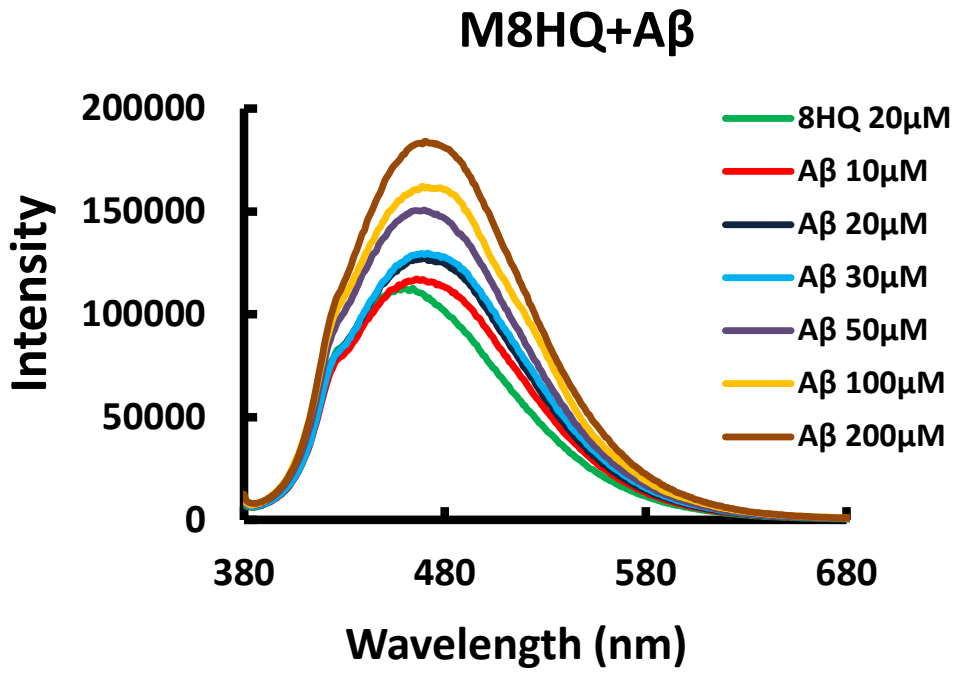

Figure S5: Fluorescence study of 20 µM M8HQ with Aβ40 monomer at different concentrations (10 to 200 µM).

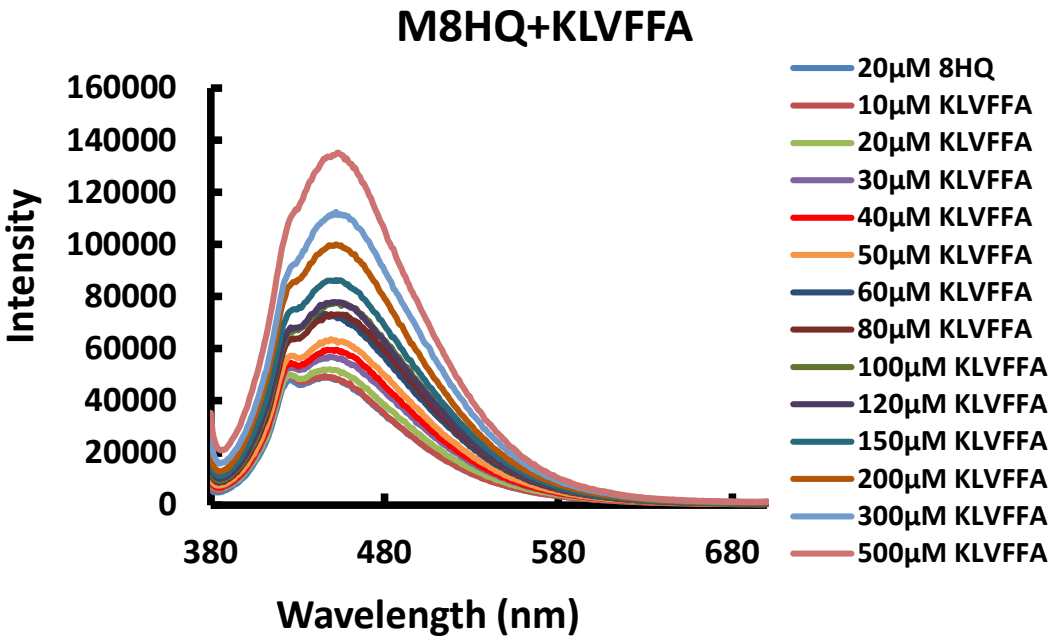

Figure S6: Fluorescence study of 20 μM M8HQ with Aβ16-21 (KLVFFA) at different concentrations (10 to 500 μM).

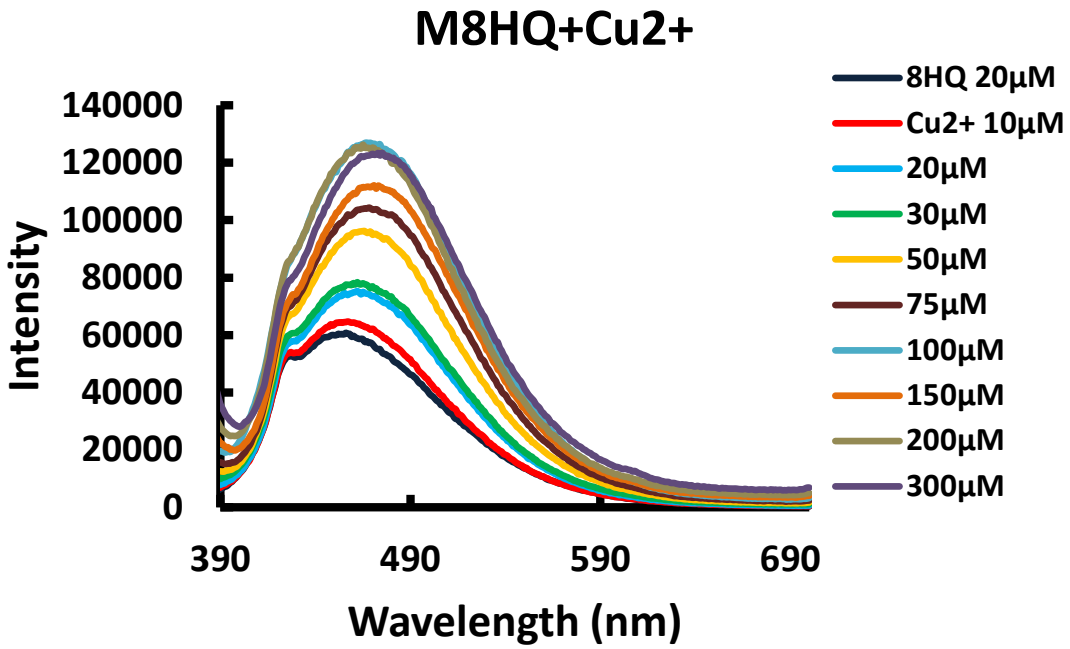

Figure S7: Fluorescence study of 20 μM M8HQ with Cu^{2+} at different concentrations (10 to 300 μM).

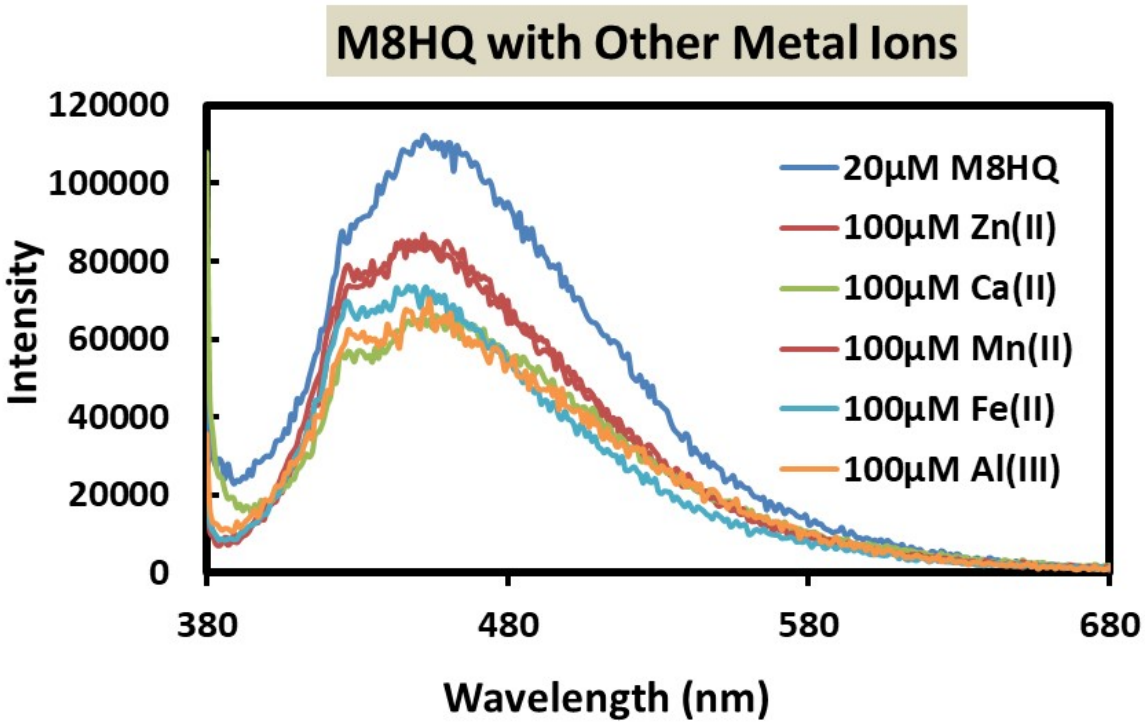

Figure S8: Fluorescence study of 20 µM M8HQ with different metal ions.

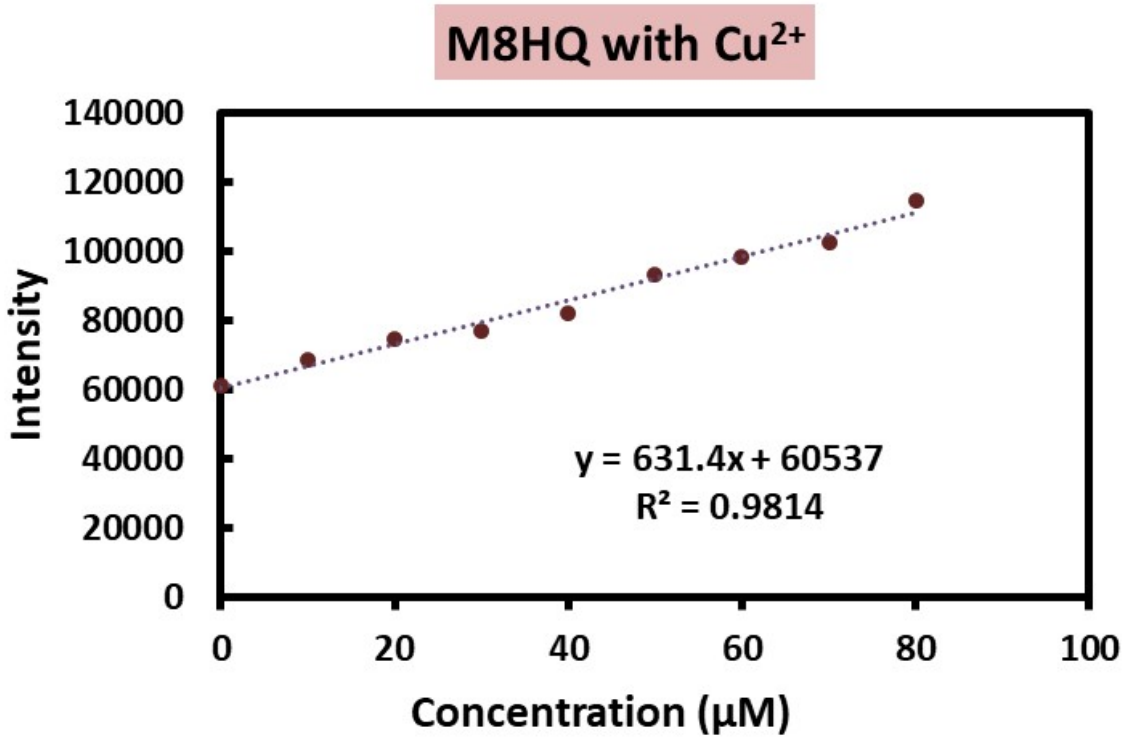

Figure S9: The limit of detection (LOD) was found 900 nM from the fluorescence study of 20 µM M8HQ with Cu^{2+} at various concentrations. (σ = 191.18 and slope = 631.4)

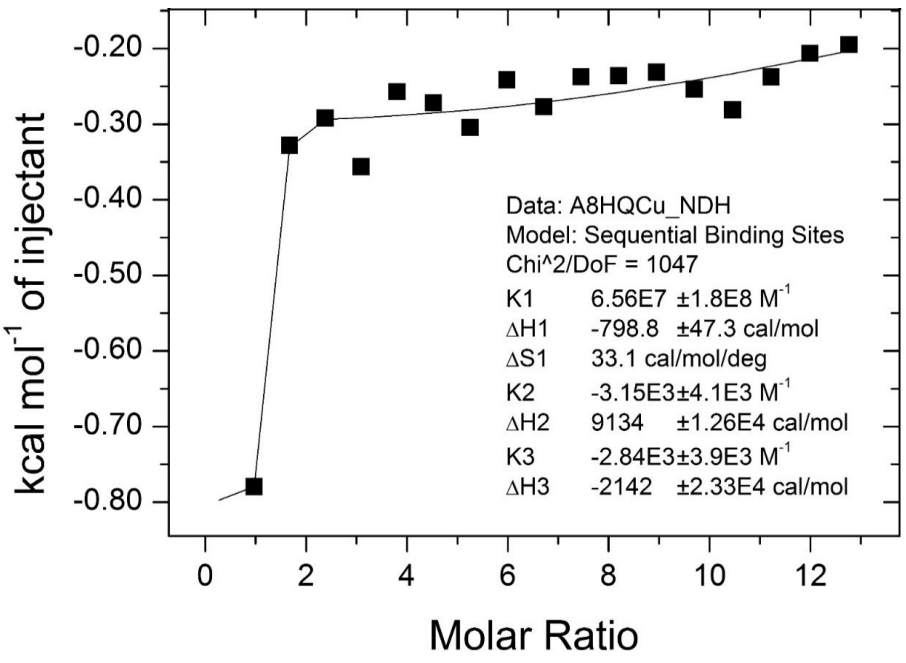

Figure S10: ITC study of M8HQ with Cu^{2+}.

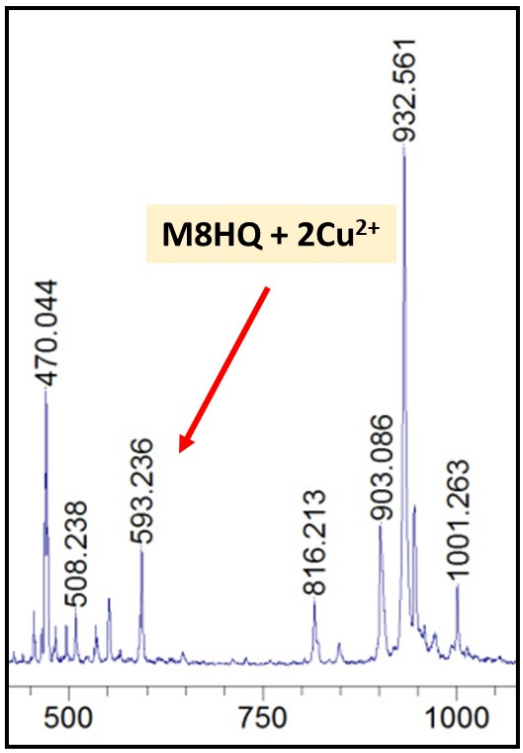

Figure S11: MALDI spectra of M8HQ with Cu(II) reveal the chelation effect and the interaction between M8HQ and Cu(II).

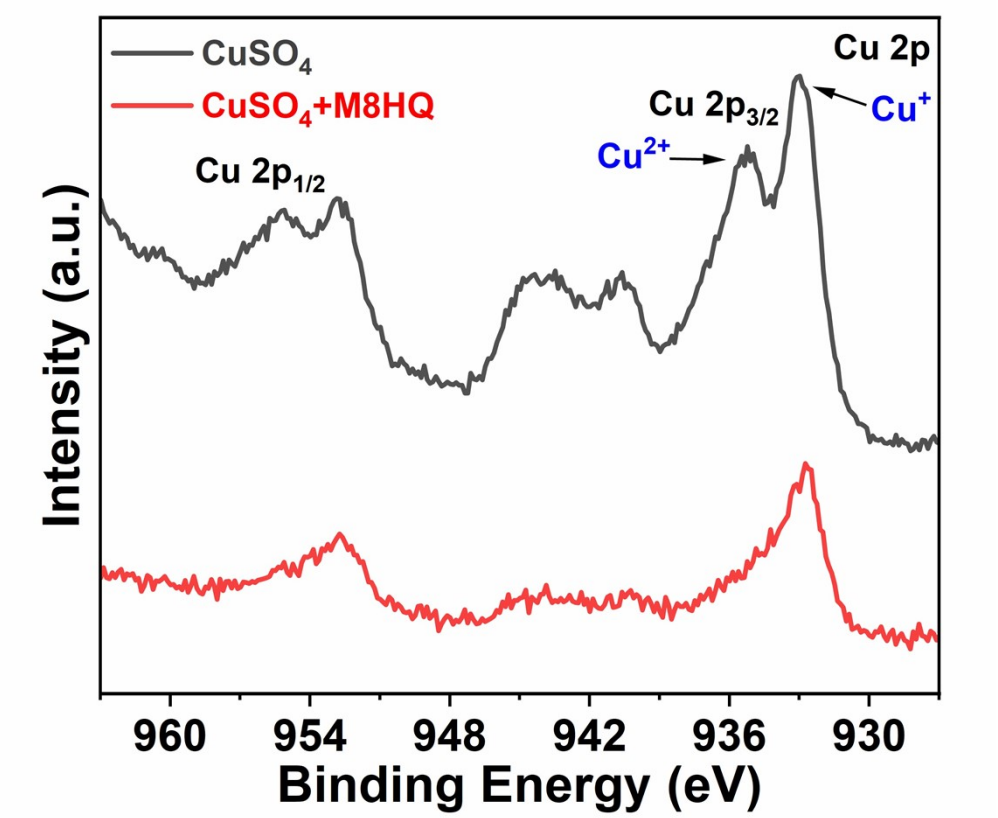

Figure S12: XPS analysis of M8HQ with Cu(II) shows the interaction between M8HQ and Cu(II).

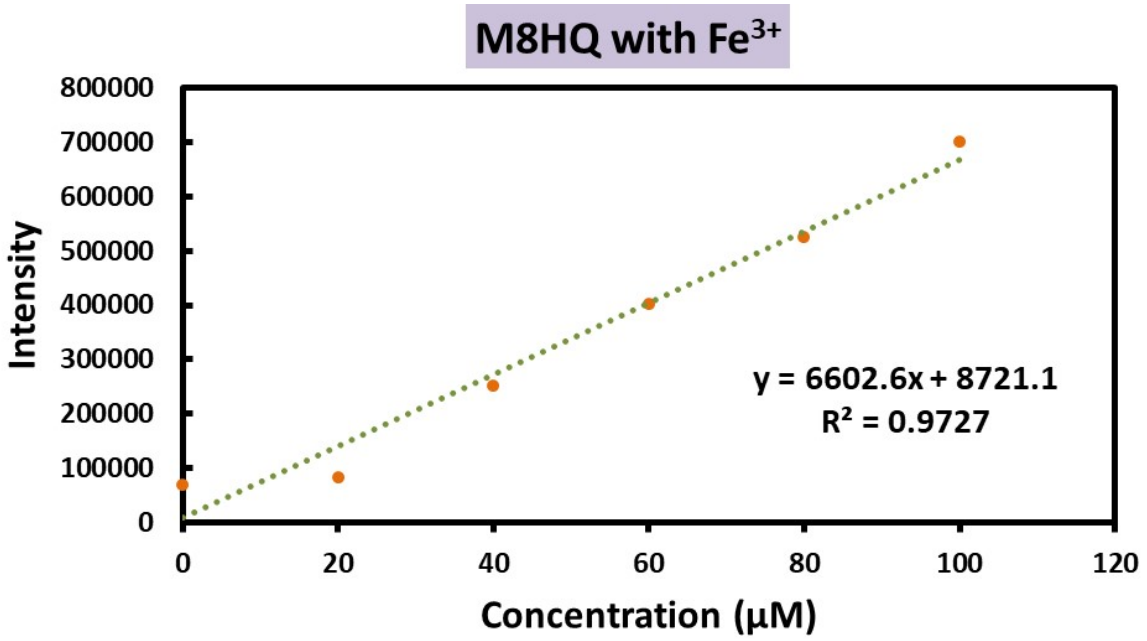

F

igure S13: The limit of detection (LOD) was found 80 nM from the fluorescence study of 20 µM M8HQ with Fe^{3+} at various concentrations. σ = 191.18 and slope = 6602)

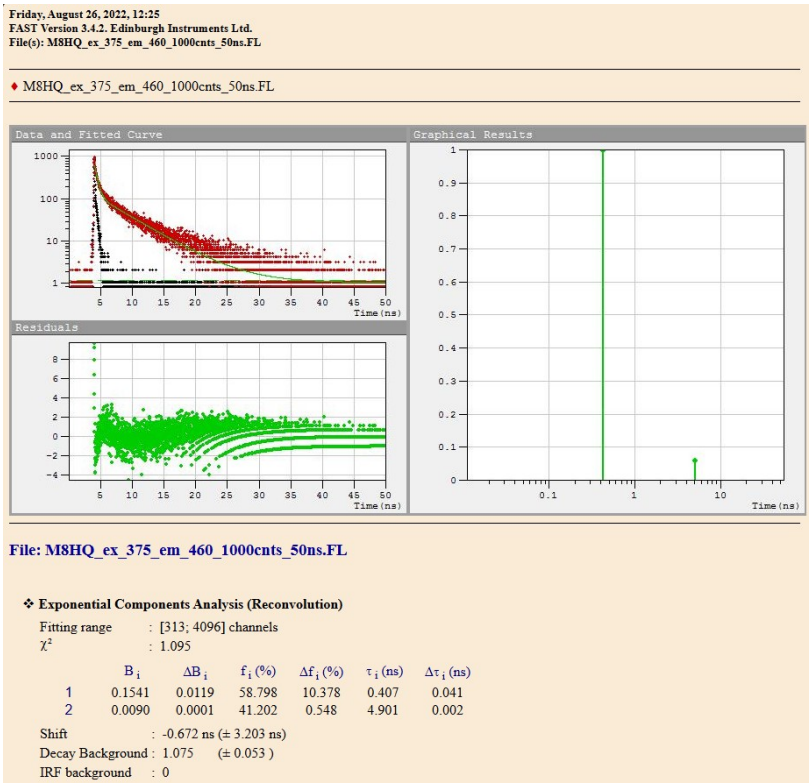

Figure S14: TRPL data of M8HQ recorded at 375 nm excitation and 460 nm emission wavelength.

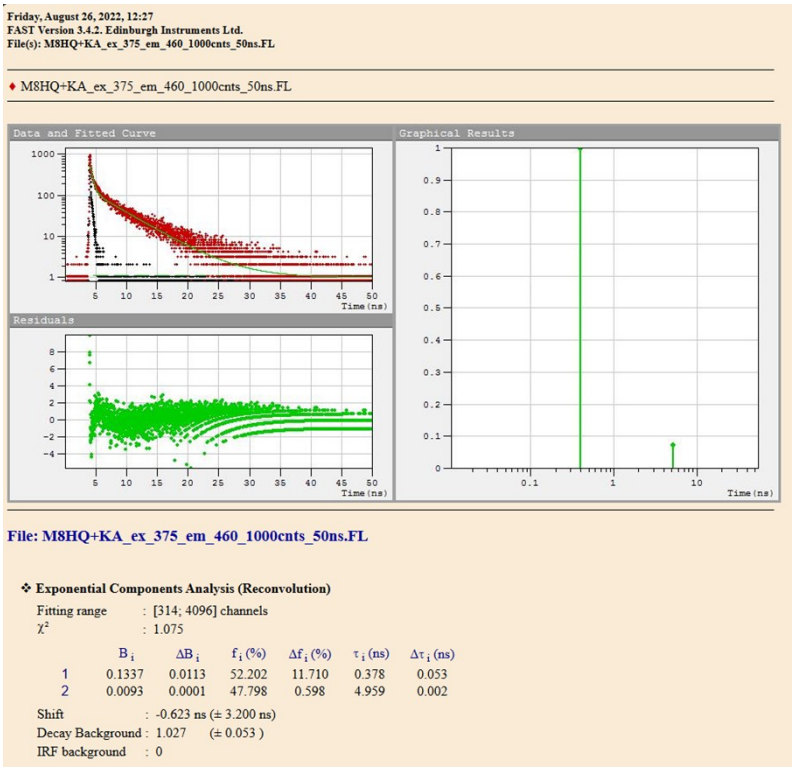

Figure S15: TRPL data of M8HQ with Aβ16-21 (KLVFFA) recorded at 375 nm excitation and 460 nm emission wavelength.

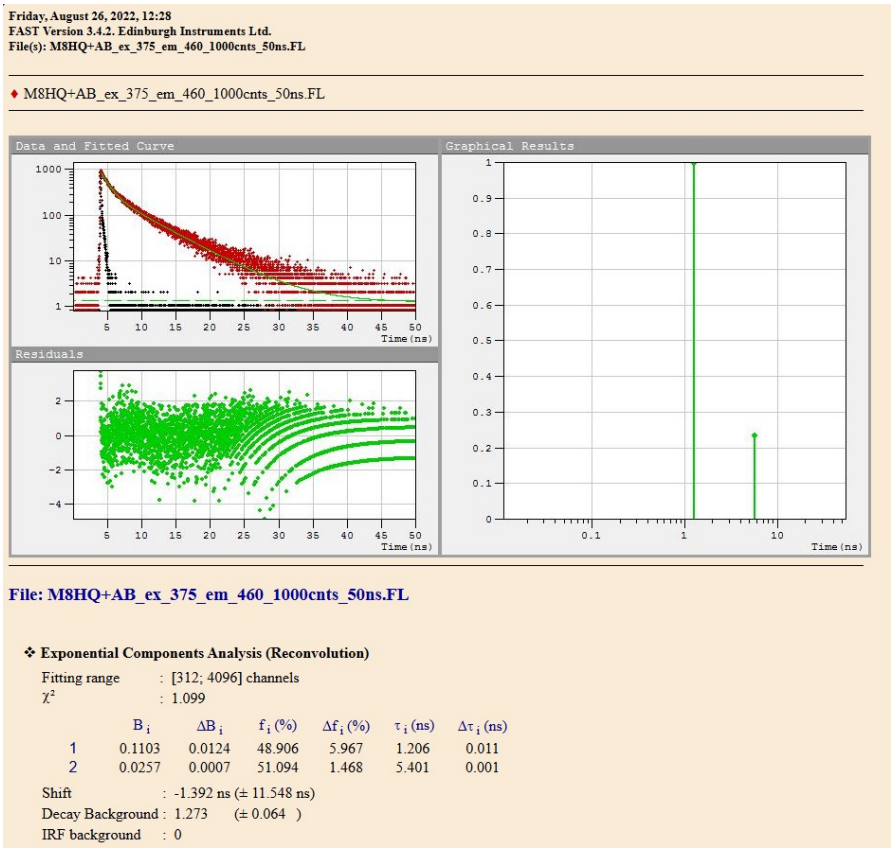

Figure S16: TRPL data of M8HQ with Aβ40 fibrils recorded at 375 nm excitation and 460 nm emission wavelength.

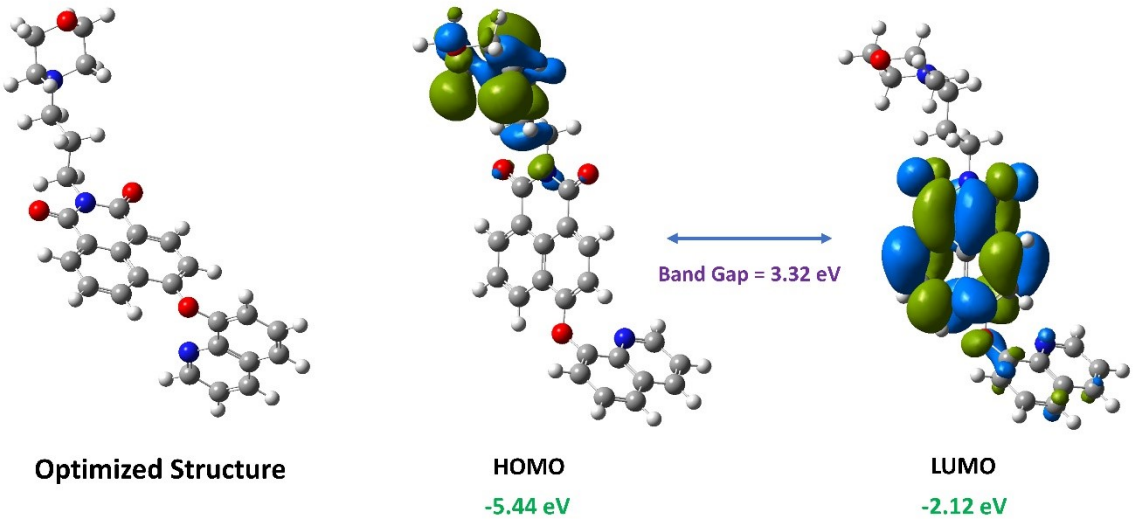

Figure S17: HOMO-LUMO and band gap determination of M8HQ using Gaussian 03 with basis set DFT, B3LYP, 631G.

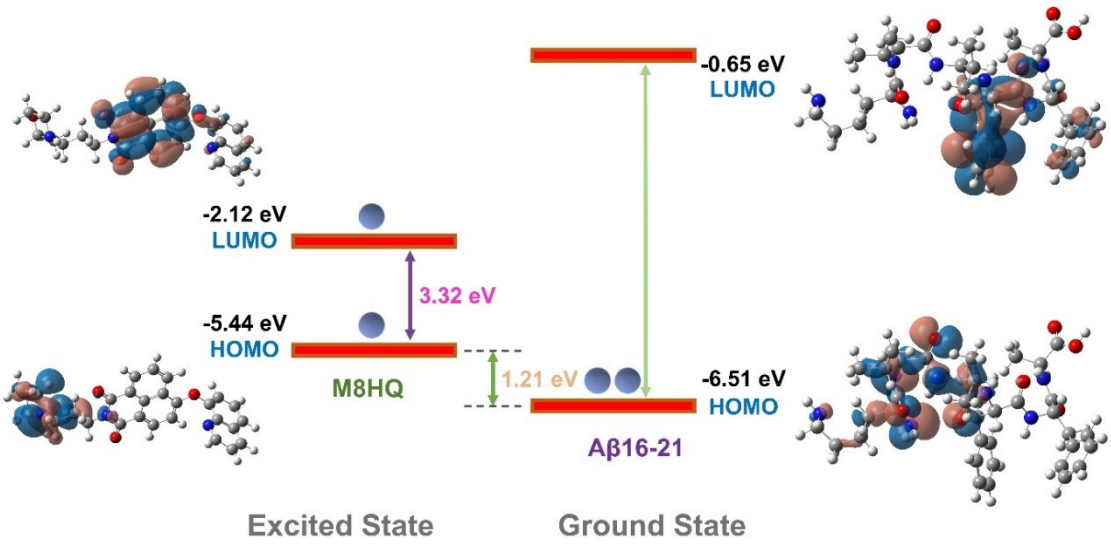

Figure S18: HOMO-LUMO and band gap determination of M8HQ and Aβ16-21 (KLVFFA) using Gaussian 03 with basis set DFT, B3LYP, 631G. HOMO-HOMO difference is 1.21 eV.

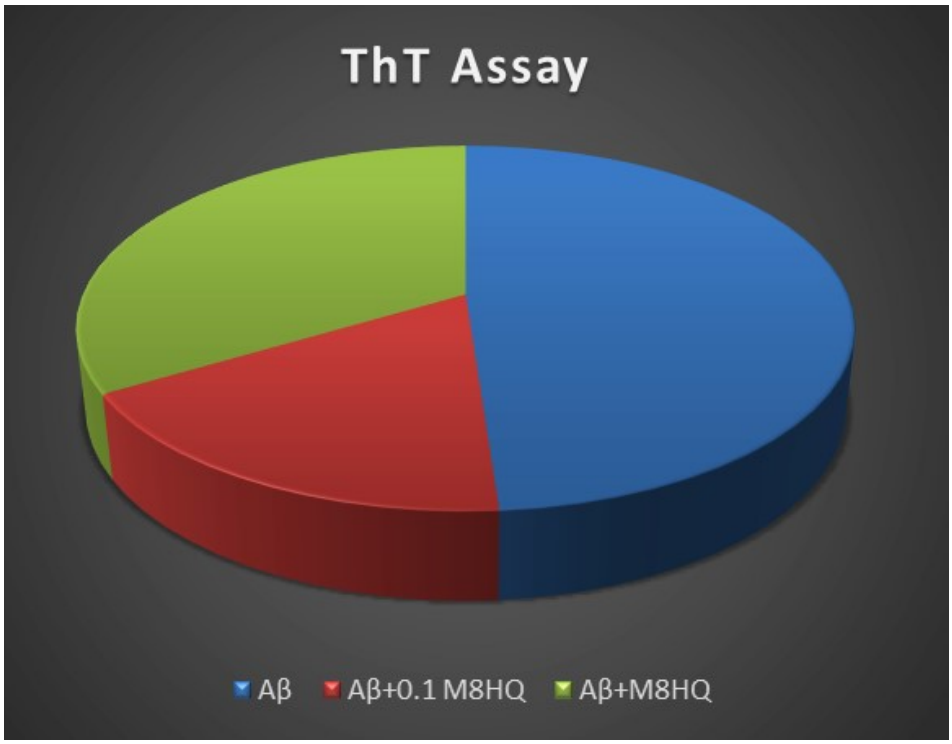

Figure S19: ThT fluorescence assay was conducted with 10 μM of Aβ40, along with two different concentrations of M8HQ: 1 μM and 10 μM. The results showed a dose-dependent inhibition of the fibrillation process of Aβ40 at 37 °C over a period of 48 hours in PBS (pH 7.4, 10 mM).

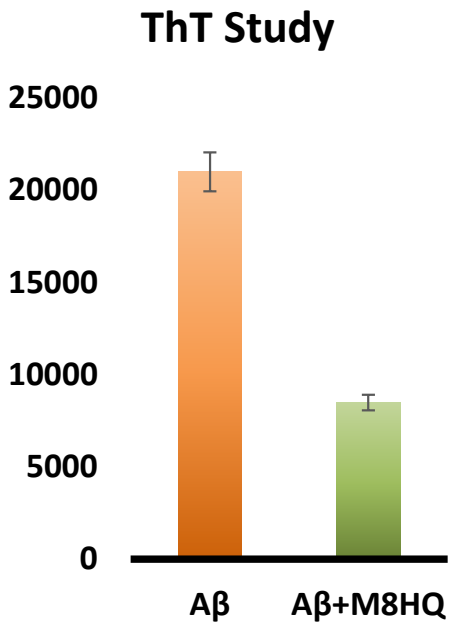

Figure S20: Disaggregation study using ThT fluorescence assay fibrillar Aβ40 and 10 µM M8HQ. M8HQ shows an instant decrease in the ThT intensity, indicating the disaggregation property of the probe.

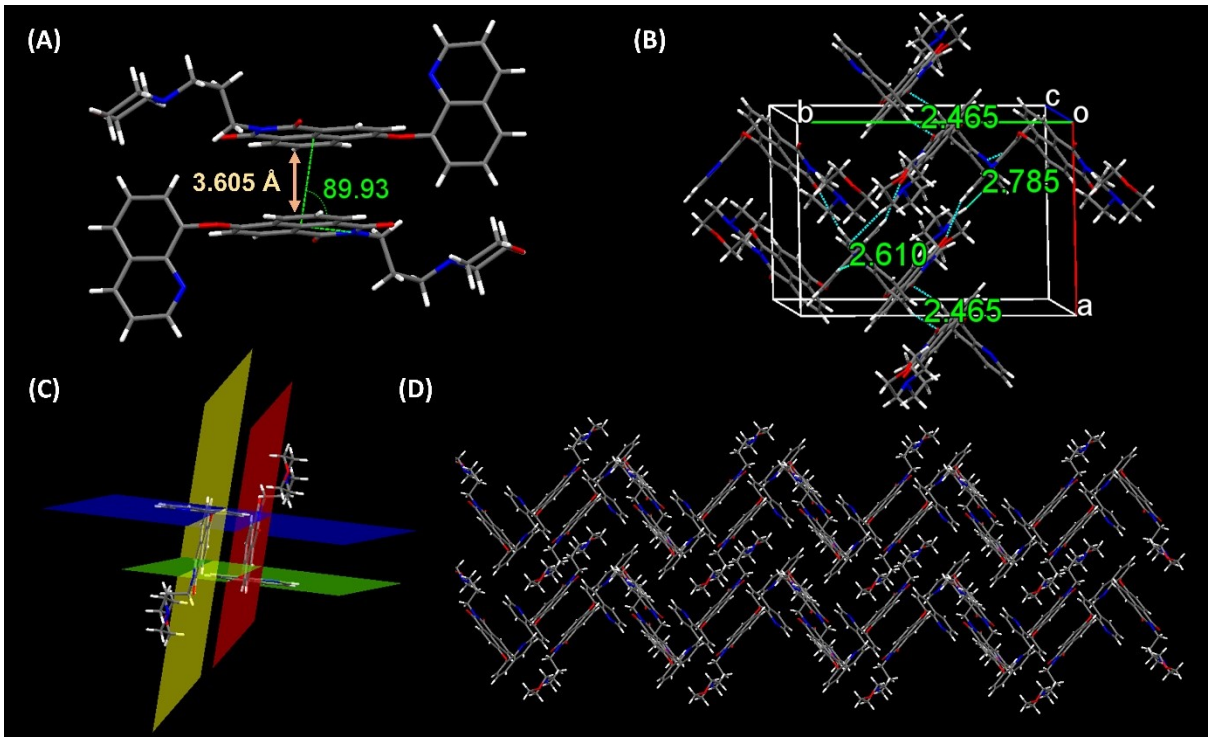

Figure S21. Crystal structure analysis of M8HQ. (A) π-π stacking interaction with a distance of 3.605 Å and an angle of 89.93°. (B) Unit cell dimensions showing intermolecular

interactions (2.465 Å, 2.785 Å, 2.610 Å). (C) Orientation of M8HQ molecules across different crystallographic planes. (D) Extended view of the periodic crystal packing arrangement.

Single crystal data and parameters of the obtained M8HQ molecule's crystal

CCDC	2374847
Empirical Formula	C28 H25 N3 O4
Formula Weight	467.53
Temperature	296 K
Wavelength	0.71073
Crystal System	monoclinic
Space Group	P 21/c
Unit Cell Dimension	a = 11.5459(12) b = 16.4083(15) c = 12.9799(12) alpha = 90 beta = 102.839(10) gamma = 90
Volume	2397.5(4)
Z	4
Absorption coefficient	0.091
Crystal density diffraction	1.317
F_000	1000
Theta range for data collection	2.47-28.85
Index Range	-13<h<13 -18<k<19 -8<l<15

Table S1. Crystal structure analysis table of the M8HQ molecule.

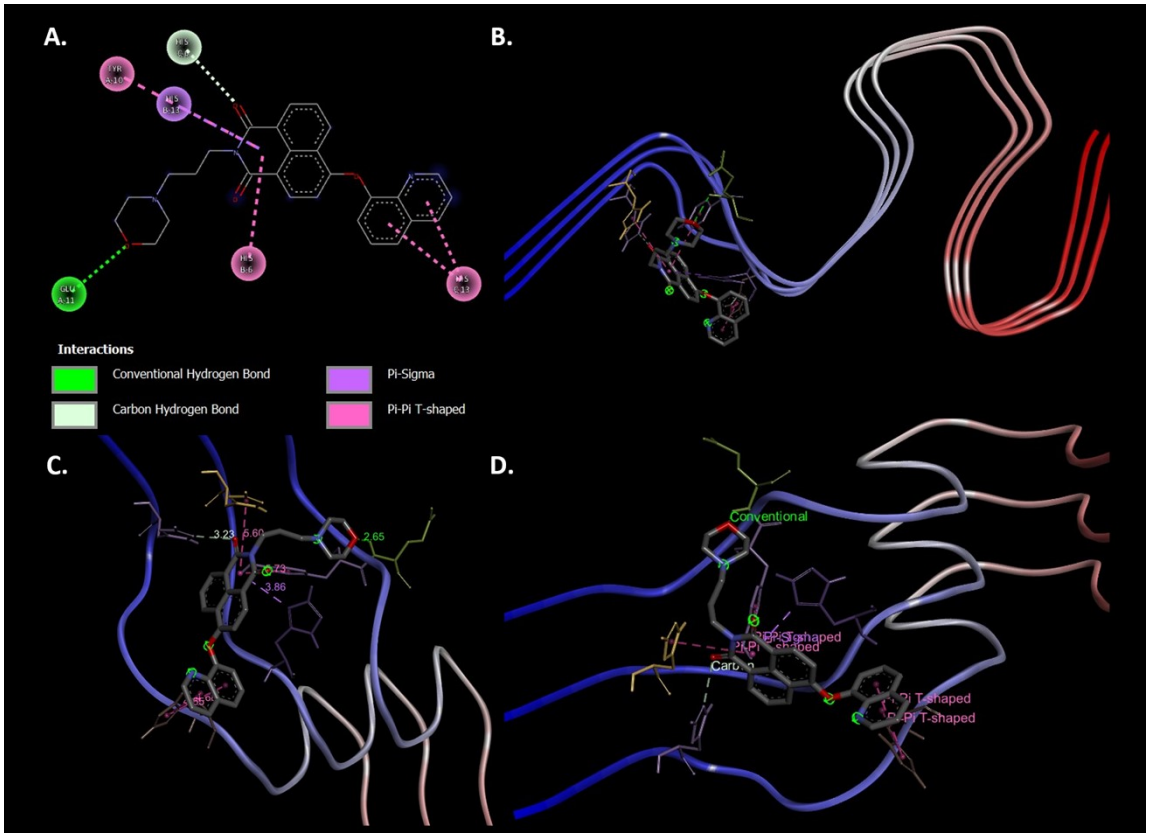

Figure S22: Molecular Docking analysis of M8HQ with Aβ42 (PDB ID: 2NAO), Estimated Free Energy of Binding = -7.35 kcal/mol, Estimated Inhibition Constant, K_i = 4.08 µM (micromolar) [Temperature = 298.15 K]

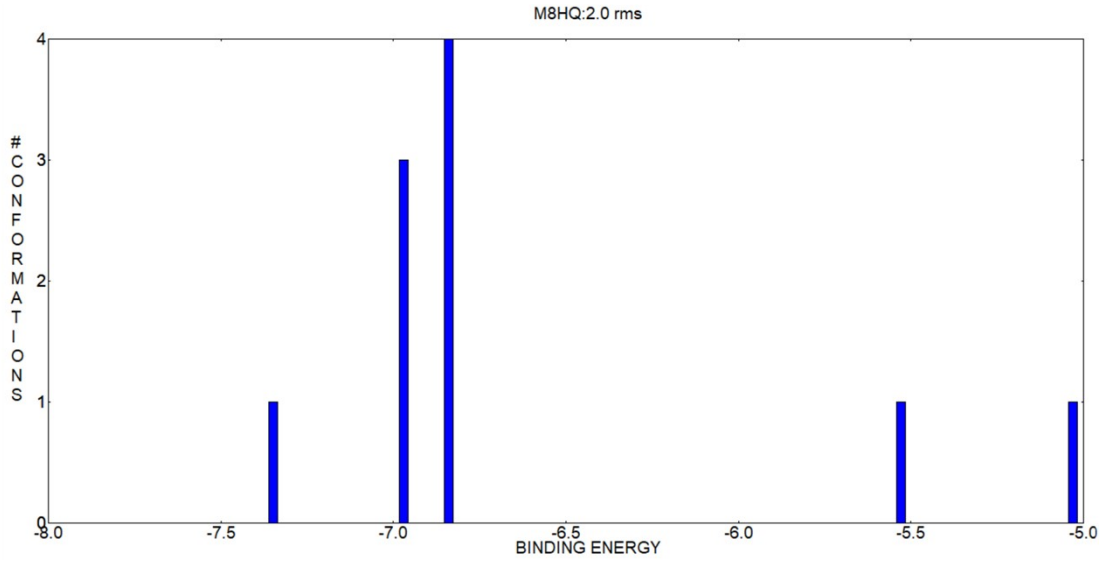

Figure S23: Cluster analysis of the binding mode of M8HQ molecule to Aβ42 (PDB ID: 2NAO), showing most of the binding structure has a binding affinity of more than -6.8 kcal/mol.

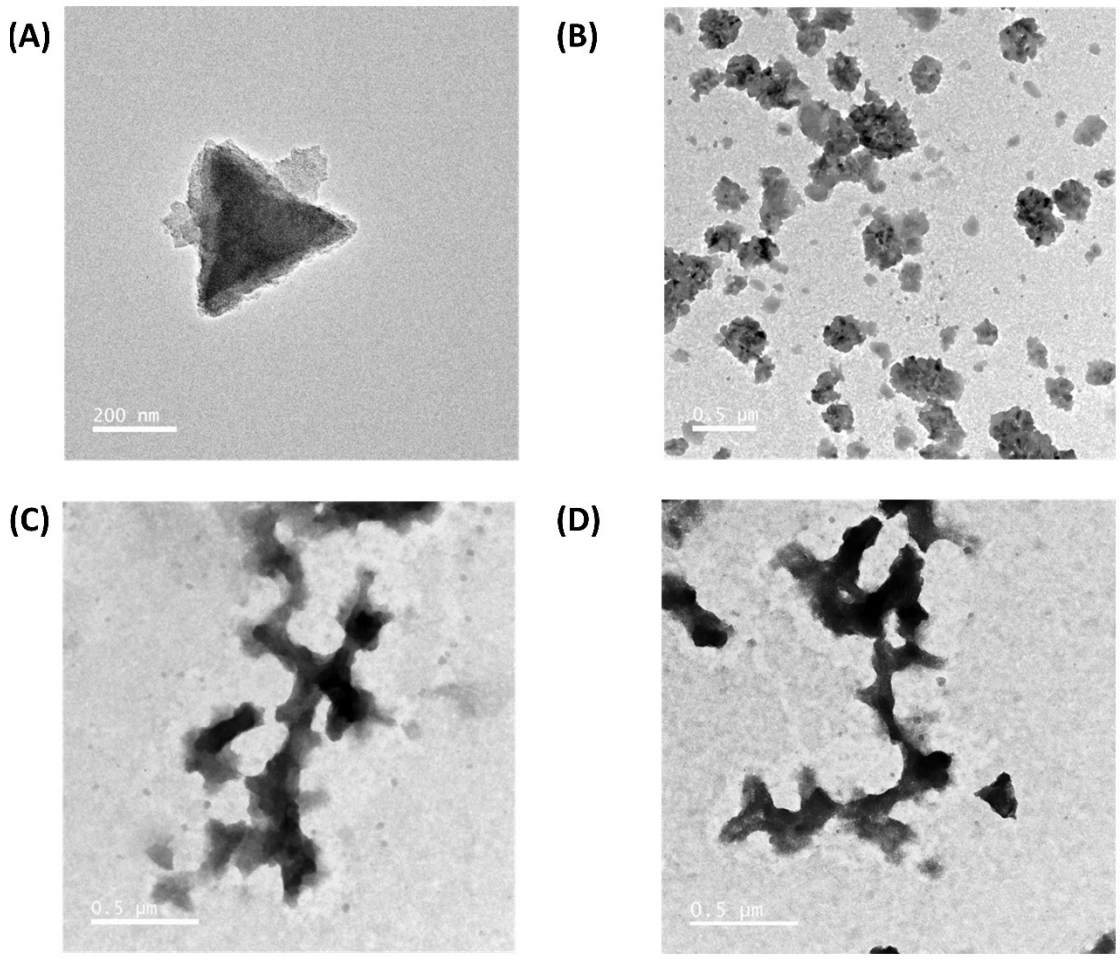

Figure S24: TEM images of M8HQ with Aβ40 (A, B) show larger aggregates formed by the M8HQ molecule at higher concentrations. (C, D) Aβ fibrils incubated with M8HQ result in a disrupted structure.

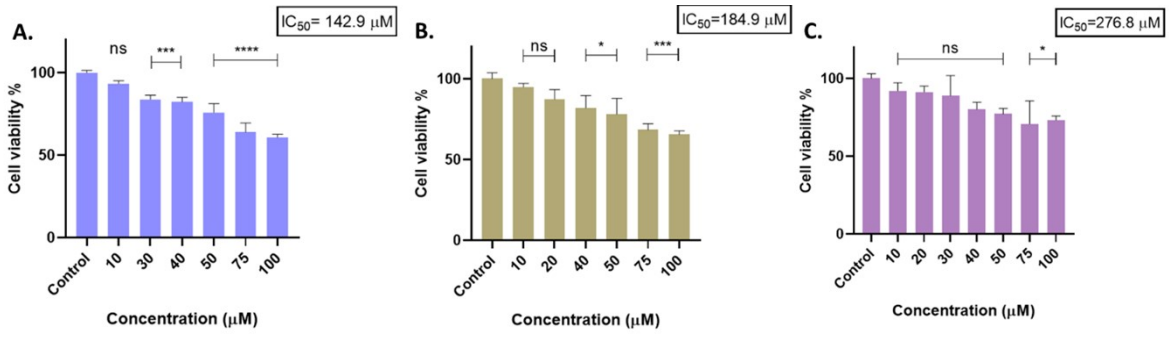

Figure S25: Cell viability assay of M8HQ at different concentrations in A. HeLa, B. HEK 293 and C. IMR 32 cell line, respectively.

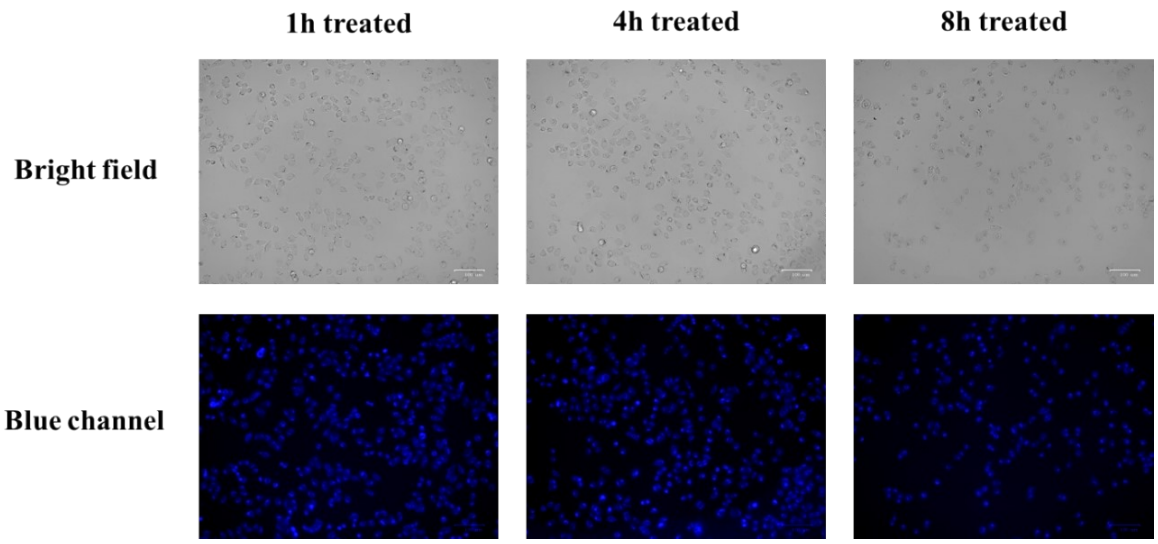

Figure S26: Cellular uptake study of M8HQ compound in IMR32 cells in 1h, 4h, and 8h.

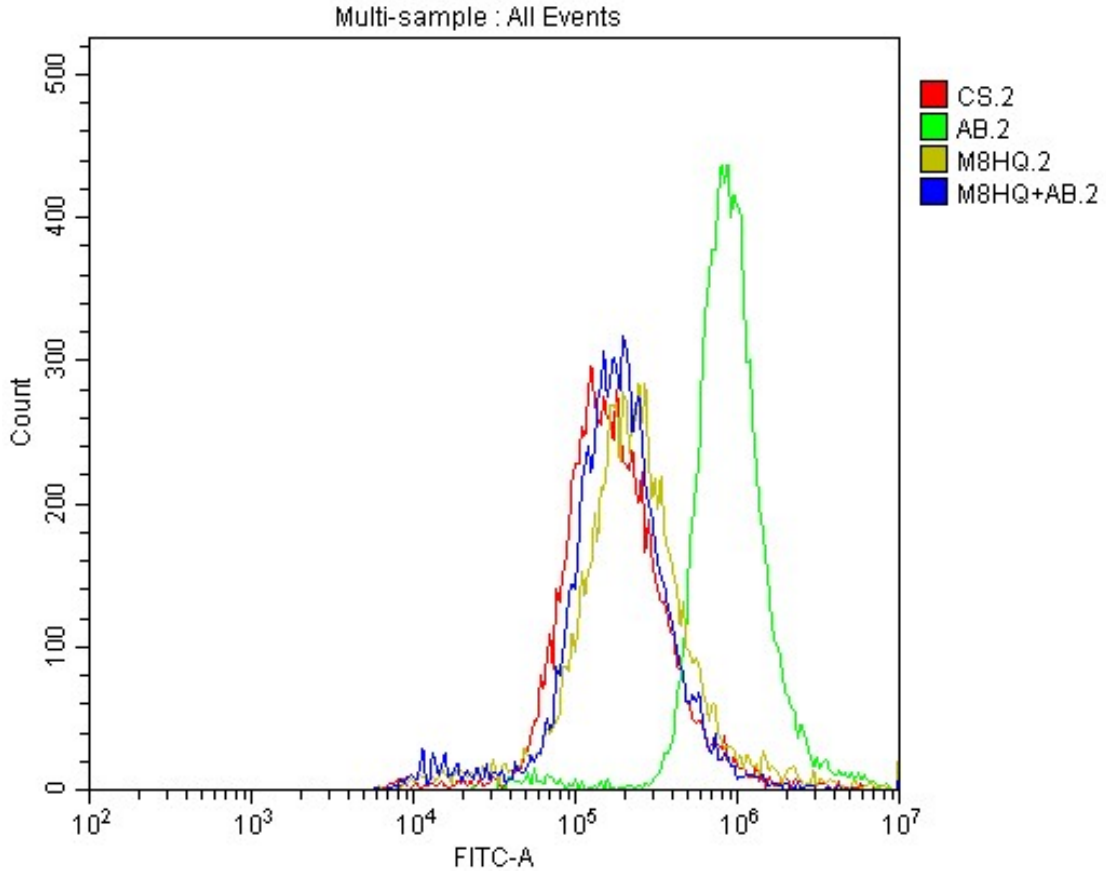

Figure S27: FACS analysis of control, Aβ40, M8HQ and Aβ40 with M8HQ compound in IMR32 cells to check the ROS generation.

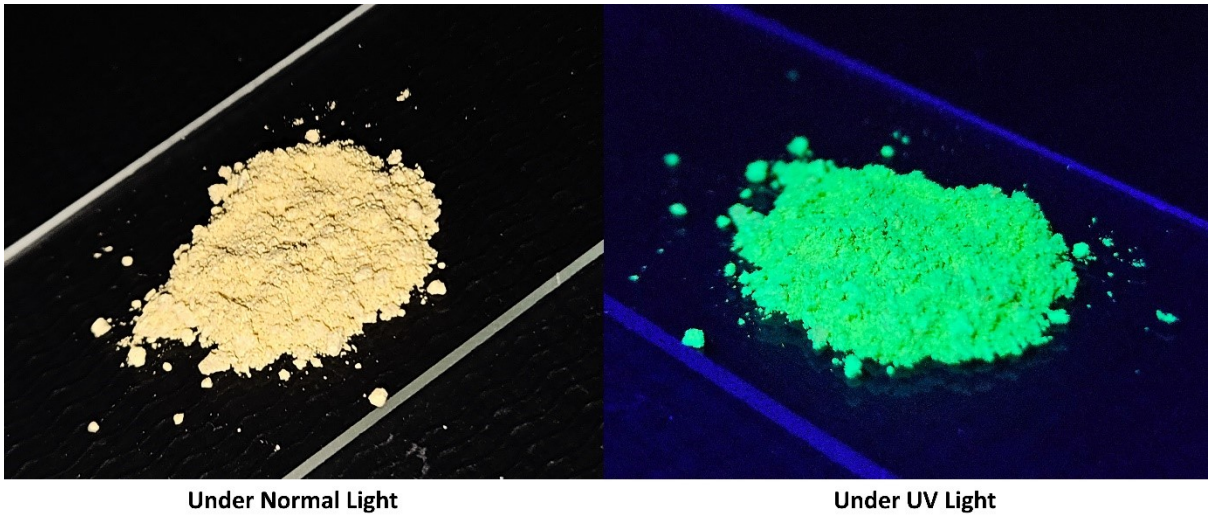

Figure S28: Photographs of the M8HQ molecule in different light conditions.

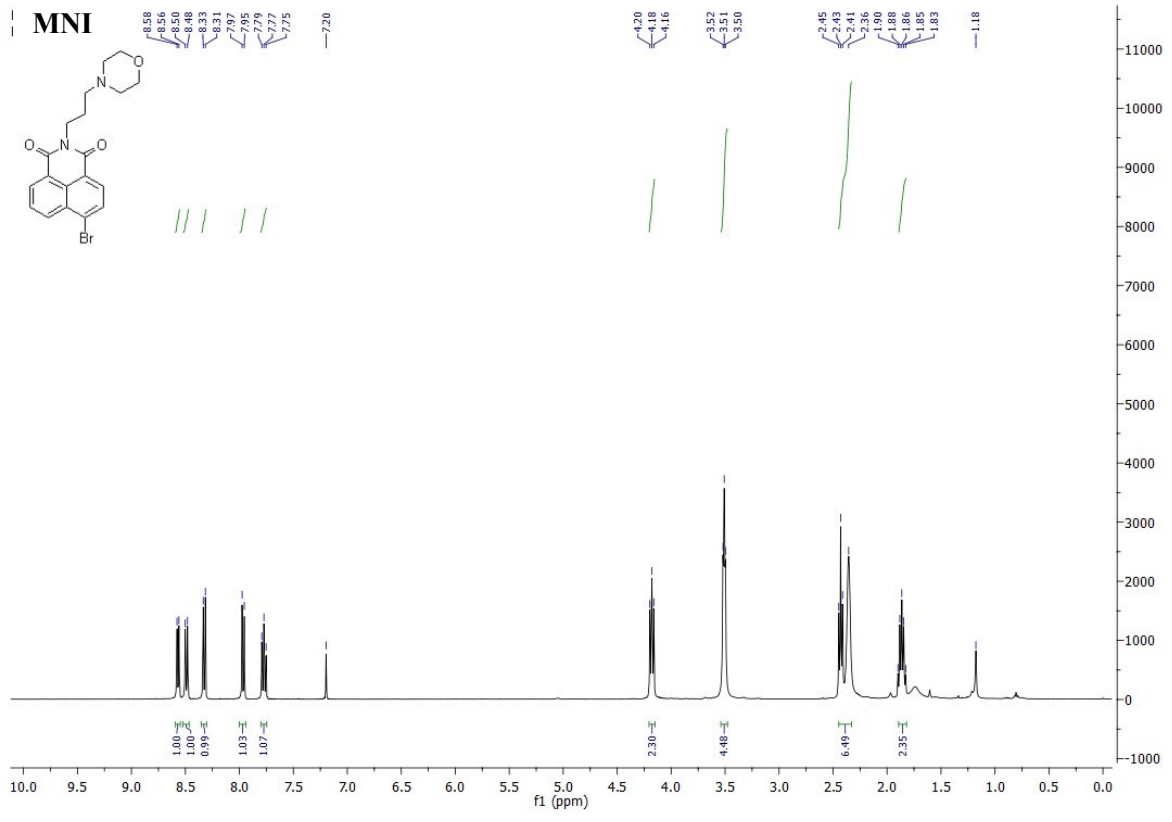

Figure S29: ^{1}H NMR spectra of MNI in $CDCl_3$

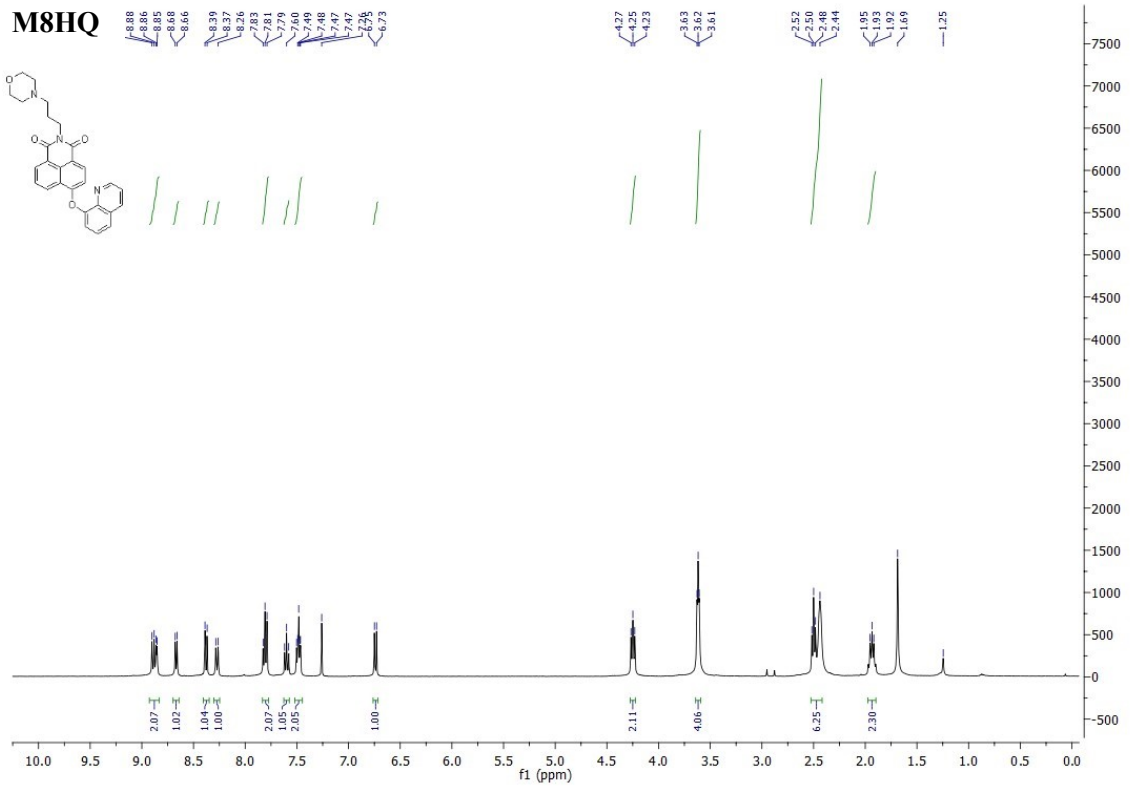

Figure S30: ^{1}H NMR spectra of M8HQ in $CDCl_3$

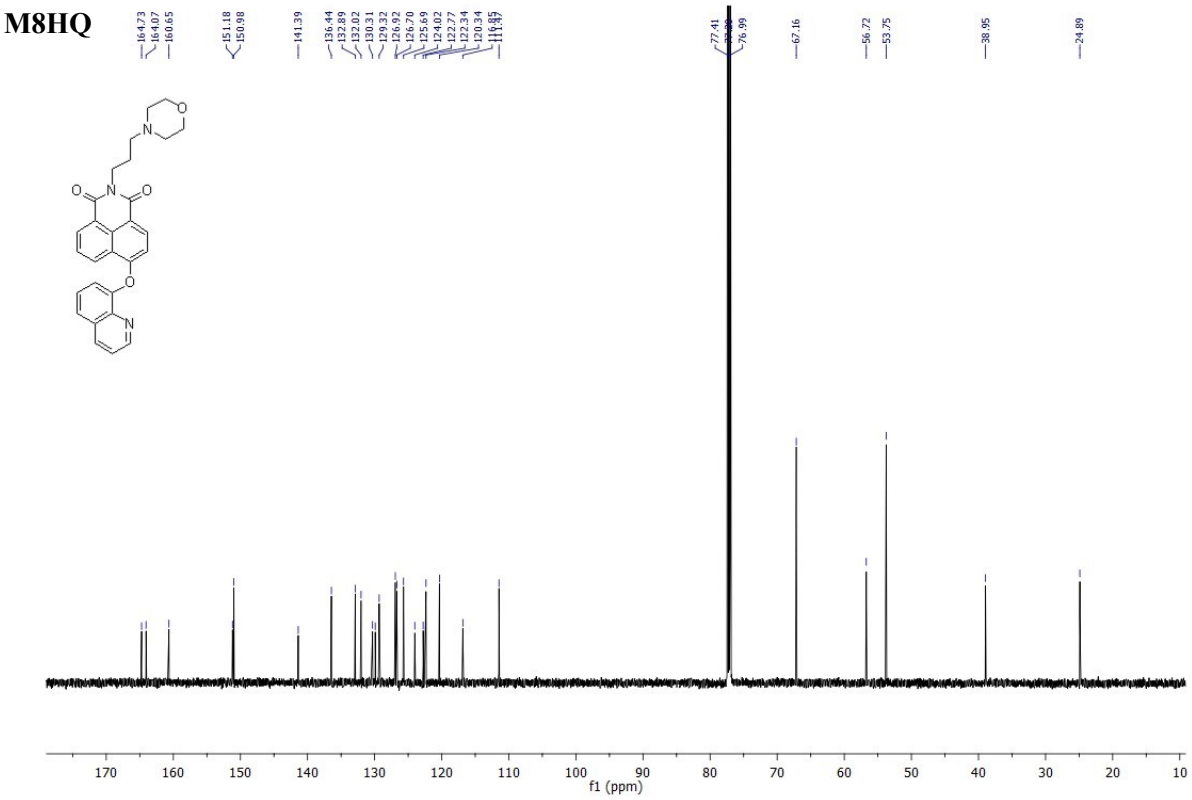

Figure S31: ^{13}C NMR spectra of M8HQ in $CDCl_3$

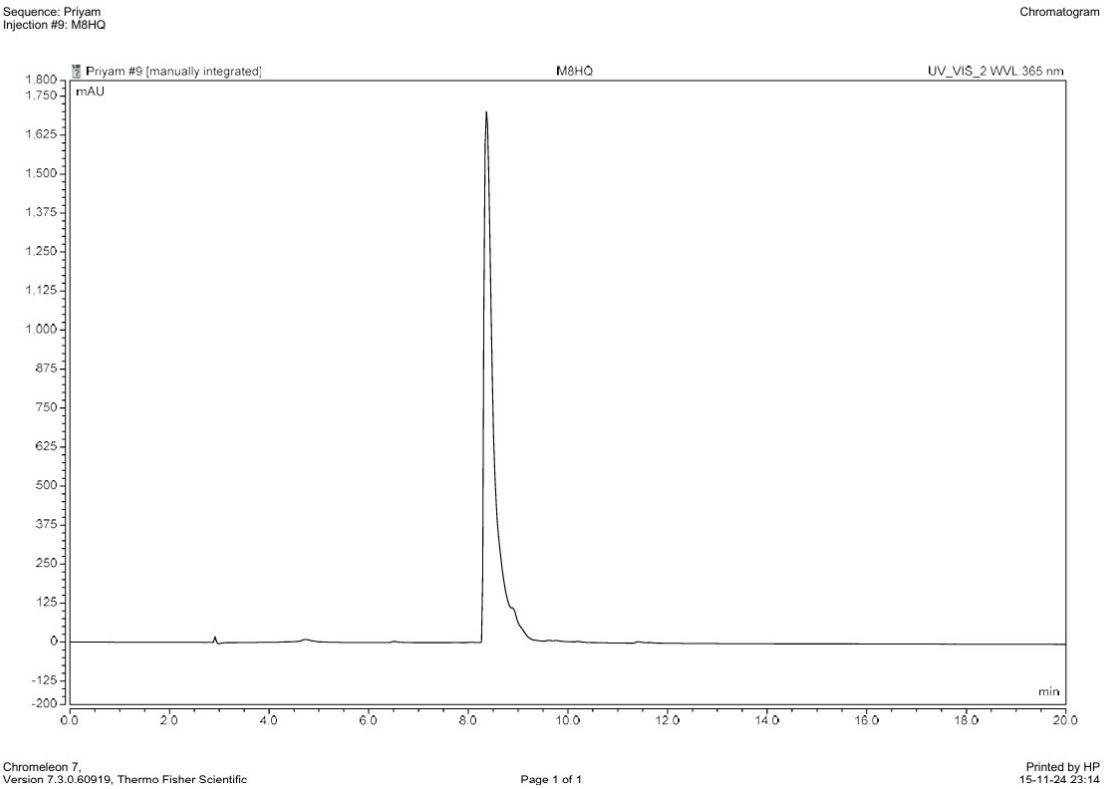

Figure S32: HPLC analysis of M8HQ at 0.5 mg/ml concentration (Water: Acetonitrile = 1:1).

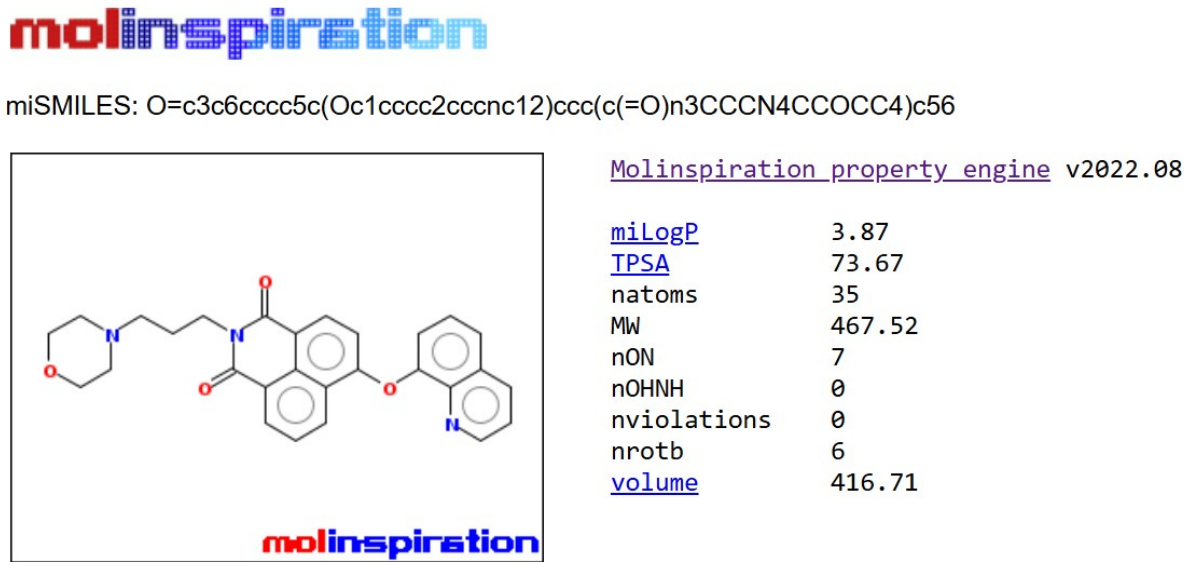

Figure S33: Molinspiration Cheminformatics Software analysis of M8HQ shows that it follows Lipinki's rule of 5.

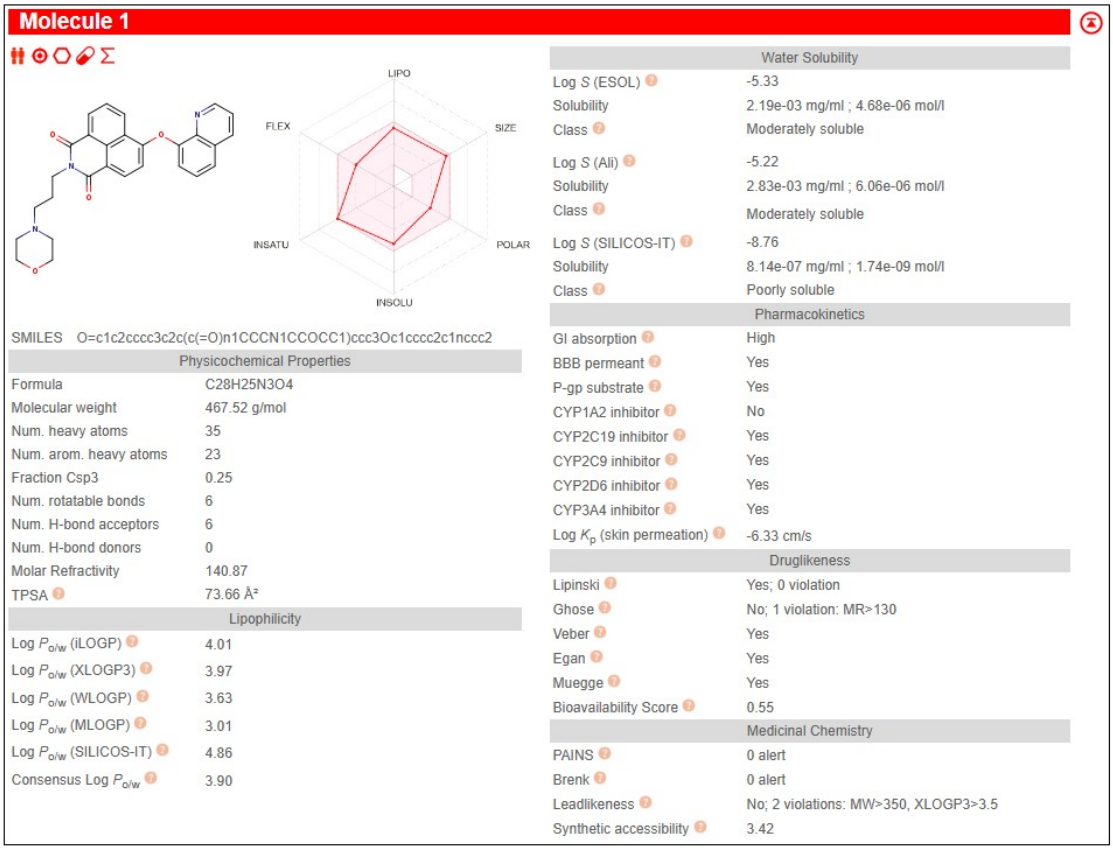

Figure S34: SwissADME Software analysis of M8HQ shows the BBB permeability prediction.

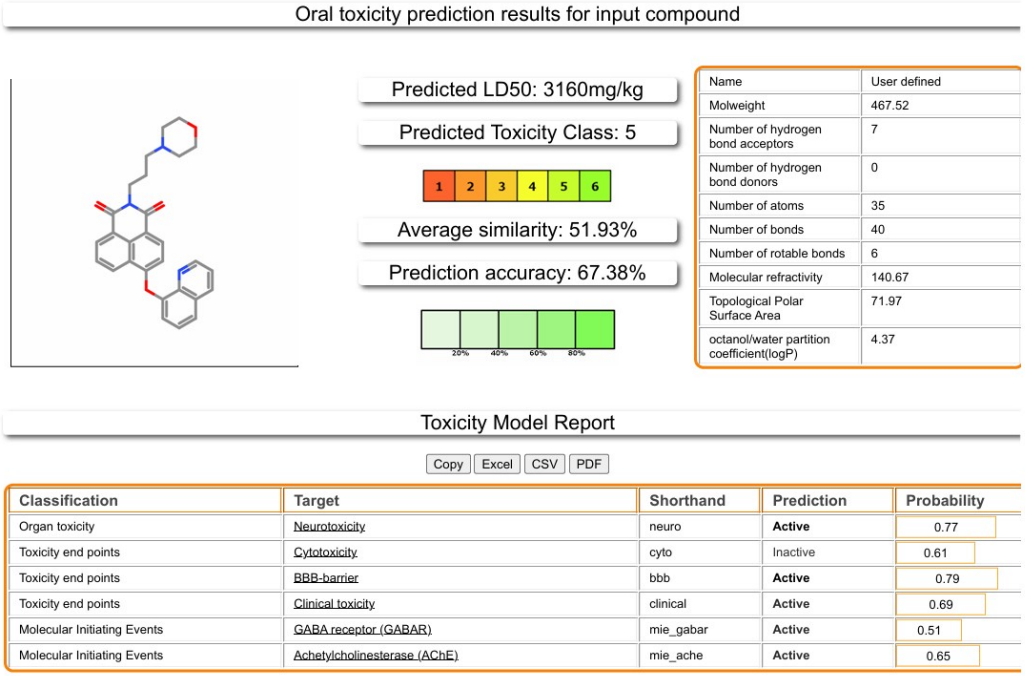

Figure S35: ProTox 3.0 Software analysis of M8HQ shows the toxicity and target prediction.